CARS2011

Section: CARS

ID: 0342

Abstract Title:
Clinical implementation of GPU-accelerated n-way 2D/3D image registration for inter-fractional patient positioning in radiotherapy

Authors:
Steininger P.[1], Neuner M. [1], Mittendorfer C. [2], Scherer P. [2], Sedlmayer F. [1,2], Deutschmann H. [1,2]
[1]ParaceIsus Medical University (PMU), Institute for Research and Development on Advanced Radiation Technologies (radART), Salzburg
[2]Landeskrankenhaus Salzburg, University Clinic for Radiotherapy and Radio-Oncology, Salzburg

Abstract Text:
Purpose

The spatial alignment of pre- and intra-interventional image data of a patient is an essential task in *image guided radiotherapy (IGRT)*. Rigidly registering the planning CT with 2D projective images (kV radiographs, MV portal images) or 3D cone beam CT (CBCT) captured each session before starting the treatment session enables the *correction of inter-fractional patient misalignments*. Daily IGRT-based patient setup correction justifies the reduction of target volume safety margins, thereby decreasing normal tissue complication probabilities (NTCP) and potentially increasing tumor control rates (TCP) if higher doses are applied.

Using one or more *2D projective images for the inference of the actual (intra-interventional) patient position* has several advantages over using 3D CBCT. These include a faster overall acquisition time, less image artifacts emerging from insufficient reconstruction algorithms, and less widespread non-target-oriented ionizing radiation deposited in the patient.

Therefore, we have used a manual projection-image-driven approach for inter-fractional setup correction in clinical routine at our institution. The *silhouette and prominent features of segmented polygonal 3D structures* (e.g. skeleton, organs at risk) are projected onto the image planes of two orthogonally acquired kV radiographs. Subsequently, the linear accelerator (LINAC) operators alter the virtual couch position (3 translations) until the projected features match the implicit features observable on the radiographs. The inferred couch position is then communicated to the LINAC, and the treatment plan is irradiated. However, recent in-house studies have shown that the variability of the determined 3D couch translation vector between different LINAC operators is occasionally unacceptable. This may mainly be due to the absent support for rotational misalignments, and too much space for interpretation.

In order to reduce observer-dependent effects on the registration, we present a *fully automatic registration framework* which is capable of registering an arbitrary number of clinical intra-interventional 2D projective images with a pre-interventional 3D CT image.

Methods

Basically, the problem of registering N 2D images $X_{R,i}, i=1..N$ with a 3D image X_M can be defined as $T_{opt}:=argmin_T \sum_i O_i \circ F_i(P_i(X_M^T), X_{R,i})$ where $P_i(X_M^T)$ are digitally reconstructed radiographs (DRRs) of the T-transformed 3D image. Moreover, $F_i(\cdot,\cdot)$ denote cost functions that compute the similarity between a DRR and the according reference image. All considered data sets are assumed being spatially positioned in a common reference coordinate system. The registration aims at finding the optimal transformation T_{opt} that aligns the projections $P_i(X_M^T)$ best with the reference images $X_{R,i}$. This is achieved by viewing the registration task as an optimization problem where the sum of the cost functions is iteratively minimized with respect to the transformation parameters $\{t\}_j$ that instantiate the actual transformation T_j at iteration j. The operators O_i enable individual numeric interpretation of each view i (e.g. individual weighting). The optimization convergence speed and the transformation reconstruction accuracy are improved by utilizing $N \geq 2$ images from adequately selected viewing directions.

The described methodical framework was implemented as a software module *(UNO-2-3-REG)* in our in-house developed record-and-verify-system (see Figure 1). In order to gain a competitive registration speed, a DRR engine that utilizes the large number of parallel shading units of the graphics card (OpenGL shading language, GLSL) for ray-casting was developed. Furthermore, the module offers the following cost functions: gradient difference (GD), normalized cross correlation (NCC), normalized mutual information (NMI) and stochastic rank correlation (SRC). For numeric optimization 1+1 evolutionary (OOE) and a downhill simplex method (AMOEBA) can be chosen. Currently, a rigid transformation T is supported which is instantiated by the 3 Euler angles and 3 translation components.

Figure 1 (fig. 1): Overview of the UNO-2-3-REG registration framework and its components.

Moreover, UNO-2-3-REG implements a fully automatic script-based masking algorithm which generates binary mask images M_i

by logically pre-processing, combining and projecting specified segmented polygonal 3D structures of the investigated patient onto the reference image planes. Using the M_i, a cost function $F_i(\cdot,\cdot)$ can determine which pixels of $X_{R,i}$ contribute to similarity measure computation. The automatic determination of mask regions plays a crucial role in 2D/3D registration with clinical radiographs that include occlusions (e.g. due to positioning aids).

Results

In order to evaluate the performance of UNO-2-3-REG, 27 IGRT radiograph pairs from 9 prostate cancer patients were randomly selected. The images were acquired using the kV on-board imaging system XVI of an ELEKTA Synergy LINAC. The X-rays were downsampled to 1 mm pixel spacing (410x410 mm). All 3D CT images had a pixel spacing of 0.98x0.98x2.5 mm and comprised the pelvic region. A masking script was configured to generate a mask M_i for each view by considering the automatically segmented skeleton (pelvis and femora) and the manually delineated planning target volume of the tumor. The script-pipeline involved 3D dilation, femur-extraction, and projection- as well as smoothing-steps which generated masks that contained the pelvis plus an additional margin, but without femora in order to prevent misregistrations due to differing hip joint positions.

For each image pair the registration started at the planned position (see Table 1.a). In a first stage, the transformation was globally initialized using the NMI cost function (without any masks) and an aggressively configured OOE optimization for 50 iterations. In the second stage, the registration was resumed utilizing the automatically derived mask images, AMOEBA optimization and 4 different cost functions (GD, NCC, NMI, SRC) in order to compare the performance. SRC was configured to extract 50 % of the pixels. Table 1.b explores the final registration results compared to the reference transformations which were manually determined by a medical expert. It shows the mean and standard error, minimum, median, 0.9-quantile, and maximum of the target registration error (TRE) related to the treatment plan isocenter, as well as the average registration time and required number of iterations. All computations were performed on an Intel Dual Core CPU 2.44 GHz, 8 MB RAM with an NVIDIA GTX 280 graphics card.

Table 1 (fig. 2): Summary of a) the initial errors before registration and b) the resulting errors after registration using GD, NCC, NMI and SRC respectively.

Conclusion

We developed a clinical prototype that is capable of coping with clinical X-rays due to an automated mask generation algorithm and a two-stage approach. The TREs compared to a manually derived gold standard showed that SRC was the most robust of the investigated cost functions yielding a mean TRE of 2.15 mm (+/-0.26 mm standard error) and a 0.9-quantile of 3.7 mm. These values are overall comparable with registration errors found in other publications that evaluated algorithms on phantom data. Closer inspection of some pretended misregistrations showed that the gold standard did not consider rotations sufficiently which were, however, corrected by the automatic registration.

Finally, we are confident that the registration results can be further improved by both tuning of the optimization and masking-script parameters.

fig.1

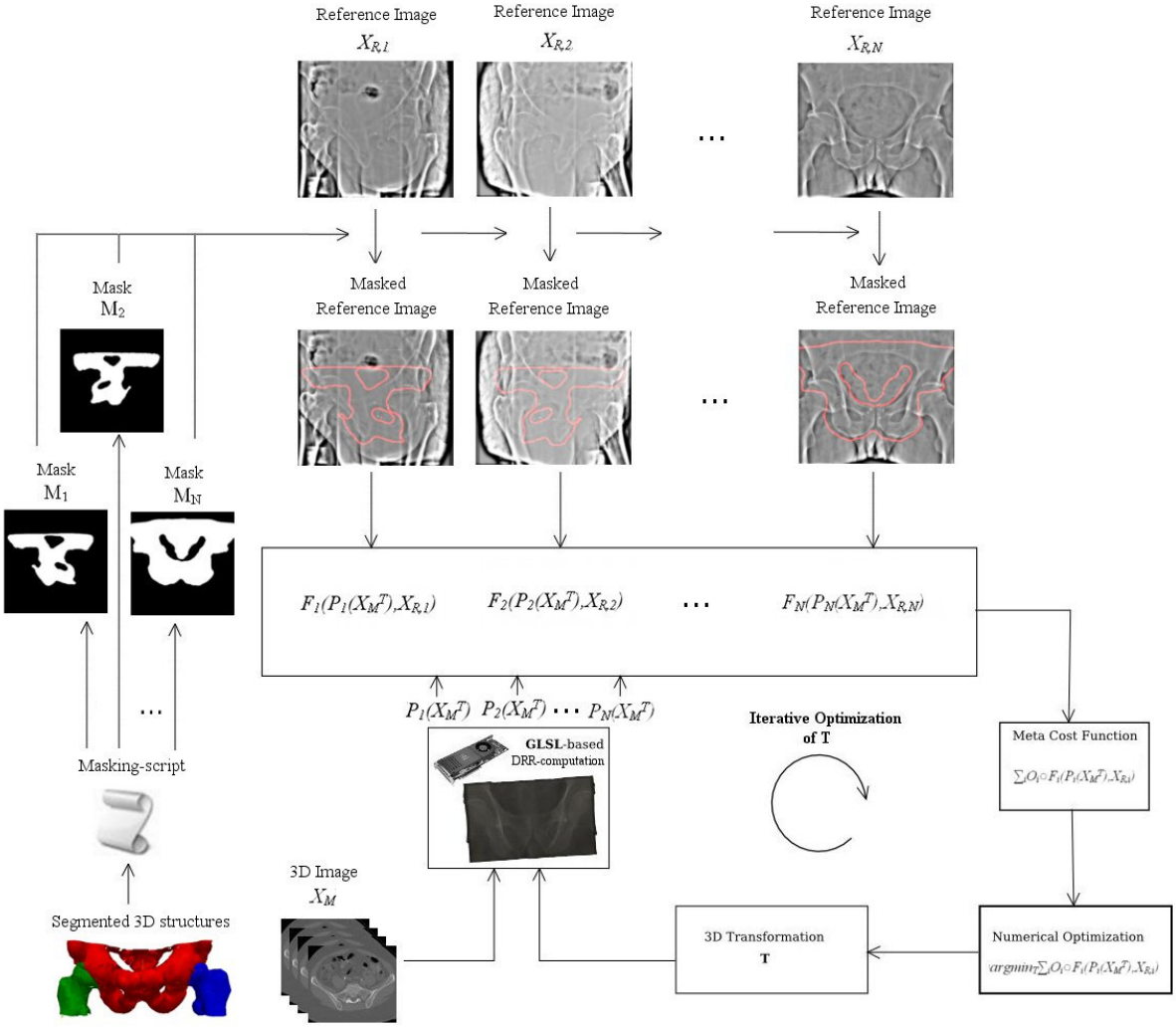

fig.2

a)

Initial TREs (N=27)			
mean+/-SE [mm]	min [mm]	median [mm]	max [mm]
6.94+/-1.61	2.43	6.41	13.61

b)

	Resultant TREs (N=27)					Time	Iterations
	mean+/-SE [mm]	min [mm]	median [mm]	Q90 [mm]	max [mm]	mean [s]	mean [1]
GD	2.40+/-0.50	0.68	2.16	4.07	7.53	24.82	141
NCC	3.17+/-2.78	0.80	1.52	7.12	15.38	17.25	147
NMI	2.93+/-0.78	0.38	2.56	5.77	7.48	9.54	73
SRC	2.15+/-0.26	0.40	1.78	3.70	5.27	10.90	110